ELSEVIER

Journal of Power Sources 112 (2002) 174–183

JOURNAL OF POWER SOURCES

www.elsevier.com/locate/jpowsour

Improvement of high-rate capability of alkaline Zn–MnO_2 battery

Chun-Chen Yang*, Sheng-Jen Lin

Department of Chemical Engineering, Ming-Chi Institute of Technology, 84 Gungjuan Road Taishan, 243 Hsien, Taipei, Taiwan, ROC

Received 29 April 2002; accepted 15 June 2002

Abstract

Electrolytic dendritic-zinc powders of high surface area are prepared from an alkaline solution by a galvanostatic electrodeposition method. The surface morphology and microstructure of these powders are examined by scanning electron microscopy (SEM) and X-ray diffraction (XRD). Cylindrical AA-size alkaline zinc–manganese dioxide (Zn–MnO_2) batteries made with powders in anode gels are assembled and tested. The electrochemical characteristics of the batteries are evaluated by means of the ac impedance method and the constant-current discharge experiments. It is found that the high-rate performance of cells with dendritic-zinc powders is much better than that of cells with conventional molten-zinc powders.

Keywords: Dendritic-zinc powder; Manganese dioxide; Impedance; Battery; High-rate discharge

1. Introduction

Commercial, alkaline zinc–manganese dioxide (Zn–MnO_2) batteries are in demand because they are mercury-free and have a high-rate capability. The primary alkaline Zn–MnO_2 battery still remains widely used in variety of applications and devices. Although various types of such batteries are available in the market, difficulties with the zinc electrode, namely, gas evolution, corrosion of zinc powder and restricted, the high-rate and high-power capability, have not been completely resolved. In general, the required purity of zinc or zinc alloys is 99.99% or higher. McLarnon and co-workers [1,2] have reviewed the development of both primary and secondary zinc batteries. Ravindran and Muralidharan [3] studied the cathodic process of zinc in alkaline zincate solution by gasometric and potentiodynamic polarisation methods. They found that an increase in ZnO concentration or a decrease in KOH concentration decreases the rate of hydrogen evolution. The Tafel slope of the hydrogen evolution reaction on a zinc electrode is about 124 mV per decade in 6–10 M KOH solution, the exchange current densities are $0.85-1.5 \times 10^{-9}$ A cm^{-2} [4]. Several authors [5–8] have investigated the ability of additives (surfactants, alloys, oxides) to suppress hydrogen evolution on zinc electrodes. Kordesch and co-workers [9,10] intensively studied rechargeable alkaline MnO_2 batteries ('RAM' batteries), which have been commercially available since 1993. They found that the capacity fade displayed by RAM cells is due predominant to zinc anode. The critical point is the deficiency of KOH electrolyte. Huot and Malservisi [11] have studied the high-rate capability of zinc electrodes in a primary alkaline Zn–MnO_2 cell in terms of zinc anode formulation, including zinc alloy composition and the particles size-distribution. It was concluded that the utilization of metallic zinc remained very low under the high-rate discharge condition. For a LR6 cell (AA size) containing 3.6 g zinc powders, the actual zinc material utilization is only 25% under 1A continuous discharge experiment. Cheh and co-workers [12–20] studied the effect of anode and cathode active materials and electrolyte properties on the discharge behaviour of a cylindrical alkaline Zn–MnO_2 cell in terms of a theoretical model.

The important criteria for a zinc electrode anode are as follows [21]: (i) high open-circuit voltage in the KOH electrolyte; (ii) low corrosion rate; (iii) minimum electrode polarization; (iv) high material utilization efficiency; (v) environmental by benign; (vi) lower material cost. To satisfy these above criteria, highly porous and dendrite electrolytic zinc powders have been prepared. In this study, characteristic properties of electrolytic zinc powders have been studied by means of scanning electron microscopy (SEM) and X-ray diffraction (XRD). Electrolytic zinc powders can also be used in many other alkaline zinc battery systems,

* Corresponding author. Tel.: +886-2-2908-9899; fax: +886-2-2904-1914.
E-mail address: ccyang@ccsun.mit.edu.tw (C.-C. Yang).

0378-7753/02/$ – see front matter
PII: S0378-7753(02)00354-3

such as Zn–AgO, Zn–Ni, and Zn–air cells, etc. An AA-size cylindrical alkaline Zn–MnO_2 cell with different compositions of zinc powder has been assembled. The electrochemical performance of the cell has been examined by the ac impedance method and the galvanostatic discharge experiments.

2. Experimental

2.1. Preparation of electrolytic dendritic-zinc powders from alkaline solution

Electrolytic solutions were prepared by dissolving a given amount of ZnO in 8 M KOH aqueous solution with the composition 6 wt.% ZnO. The electrodeposition of dendritic-zinc powder was performed out in a 500 ml two-electrode electrochemical cell. Both the working electrode and the counter electrode were nickel plate with an area of 30 cm^2 (5 cm × 6 cm). A EG&G 273A potentiostat was used to run the galvanostatic zinc deposition by varying the current density in the range of 50–250 mA cm^{-2}. The electrodeposition temperature was varied between 25 and 70 °C. After electrodeposition, the electrolytic dendritic-zinc powders were easily removed from the nickel electrode with a knife. The powders were then rinsed three times, dried, and stored in a polyethylene plastic bag to avoid further oxidation. The apparent densities of the electrolytic zinc powders were also measured by a means of standard pycnometric method.

2.2. Studies of the properties of electrolytic Zn powders by SEM and XRD

The surface morphology of 99.995% molten zinc (UM) and the electrolytic dendritic-zinc powders were characterised by using a scanning electron microscope (Hitachi S-2600 SEM). The crystal microstructures of the electrolytic zinc powders were examined by a Philip X-ray diffractometer with Cu Kα radiation of wavelength $\lambda = 1.54056$ Å for 2θ angles between 10 and 80°.

2.3. Preparation of zinc gels

Zinc gels for the anode of the Zn–MnO_2 cell were made by mixing 61–65 wt.% Zn powder, 1 wt.% gelling agent (Carbopol 940), and 0.05–0.2 wt.% of indium acetate and 31–35 wt.% of 8–9 M KOH solution containing 1–3 wt.% of ZnO. The water content in anode zinc gels was measured by means of a HR73 moisture analyser (Mettler Toledo).

2.4. Electrochemical characteristics of alkaline Zn–MnO_2 batteries

The impedance of LR6-size Zn–MnO_2 cells before and after discharge experiments were measured. Cells with different compositions of zinc powder, additives, and KOH electrolyte were assembled and kept for several hours prior to test. The ac frequency range was set between 300 kHz and 10 mHz. The impedance measurements were performed with Autolab PGSTAT40 equipment (Eco Chemei B.V., The Netherlands) and a frequency response analysis software under an amplitude of 5 mV. Nyquist plots used to interpret the electrochemical performance of the cell. In this study, each of the AA-size Zn–MnO_2 cells comprised of anode with 3.6 g electrolytic dendrite zinc-powder or molten zinc or mixture them in a gel, a EMD MnO_2 cathode, a separator, and a steel can (taken from commercial AA-size alkaline Zn–MnO_2 cells). The ac impedances of the Zn–MnO_2 cells were measured at open-circuit potential (OCV). Galvanostatic discharge experiments were performed for various cells with the different formulations of zinc gel at room temperature. The discharge currents were conducted over a range 50–600 mA at 25 °C by an automatic BAT 770 charge–discharge device. The end-of-discharge was set at 0.6 V.

3. Results and discussion

3.1. Electrolytic zinc powder

Electrolytic dendritic-zinc powders were prepared at different current densities from a 8 M KOH solution that contained 6 wt.% ZnO at temperatures of 25, 50, and 70 °C. The current density for galvanostatic electrodeposition of zinc powder was in the range of 50–250 mA cm^{-2} at static conditions. The structure of the deposit depends on the current density and mass-transfer rate of the electrodeposition system [22]. The morphology of electrolytic zinc formed at below 100 mA cm^{-2} is a fine porous powder. When the current density is above 100 mA cm^{-2}, the morphology of electrolytic zinc changes to a dendritic form. The electrode reaction of zinc electrodeposition is totally under diffusion-limited control. The higher the electrodeposition current density, the greater is the polarization of the working electrode. The current efficiency (CE) of the electrodeposition of zinc powder is in the range 51.24–84.70% when the current density varied at between 100 and 250 mA cm^{-2}. The CE values are listed in Table 1. The highest current efficiency of zinc electrodeposition is 84.70% at a current

Table 1
Current efficiency (CE) and tap densities (ρ) of electrolytic zinc powders

Current density (mA cm^{-2})	$M_{Zn,theo}$ (g)	$M_{Zn,real}$ (g)	CE (%)	ρ (g cm^{-3})
100	0.7308	0.3745	51.24	4.76
166	1.2180	0.7046	57.85	5.08
200	1.8270	1.5482	84.70	5.26
250	1.4616	1.1239	76.89	5.42

Electrodeposition for 1 h at 25 °C.

density of 200 mA cm^{-2} at 25 °C. The tap density of the electrolytic dendritic-zinc powders varied from 4.76 to 5.42 g cm^{-3}, as shown in Table 1. It is found that the zinc powders become much more porous and have a dendritic structure when the temperature or the current density of zinc electrodeposition is increased.

The current efficiencies at 25, 50, and 70 °C at a constant-current density of 200 mA cm^{-2} are given in Table 2. The higher the electrodeposition temperature, the higher is the

Table 2
Electrodeposition of zinc powder at different temperatures and a constant-current density of 200 mA cm^{-2} from 8 M KOH solution with 6 wt.% ZnO

Temperature (°C)	$M_{Zn,theo}$ (g)	$M_{Zn,real}$ (g)	CE (%)	ρ (g cm^{-3})
25	1.8270	1.5482	84.60	5.42
50	1.8270	1.6264	89.05	5.65
70	1.8270	1.7849	97.80	6.43

Electrodeposition for 1 h.

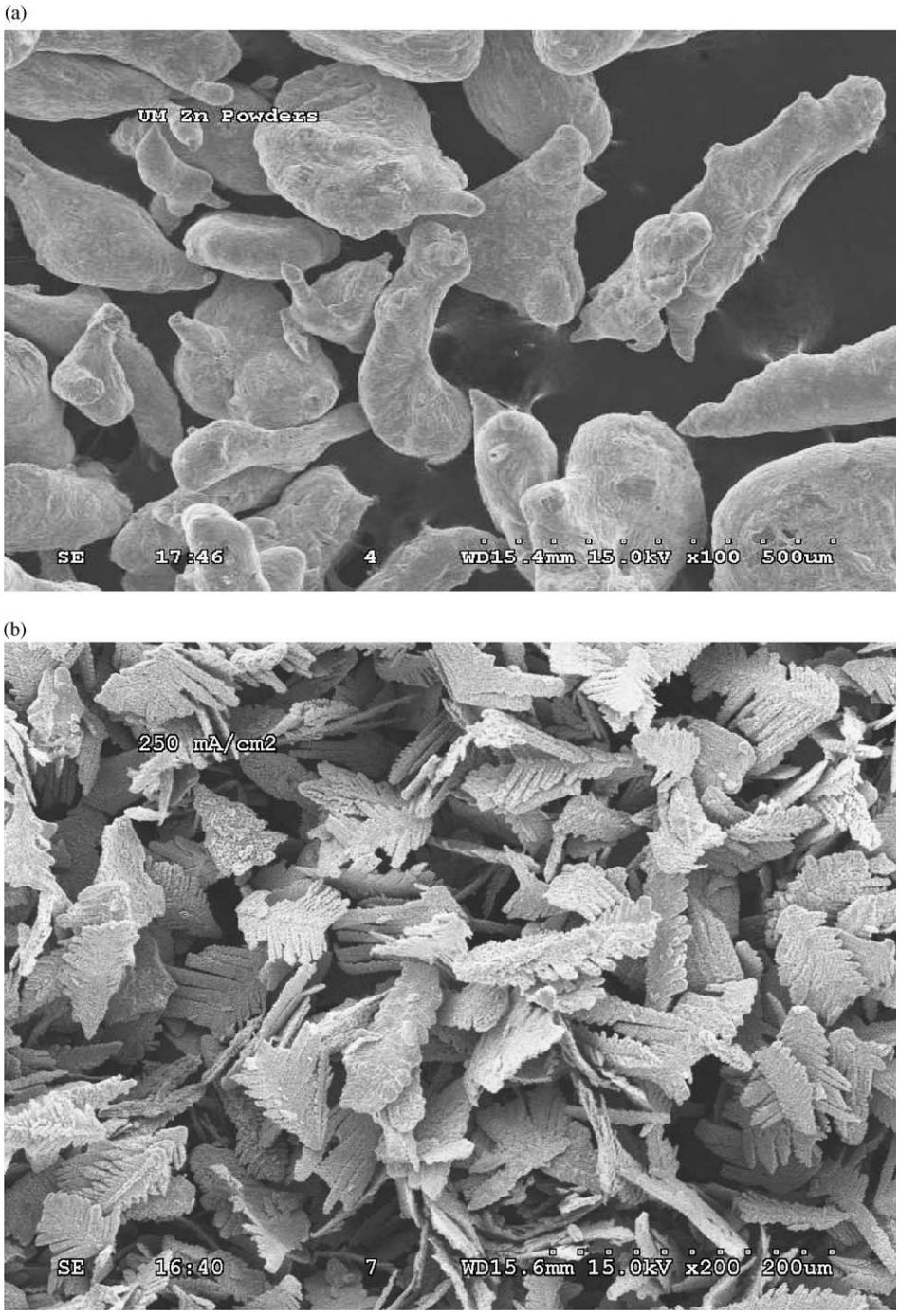

Fig. 1. Surface morphology zinc powders: (a) molten-zinc powders; (b) dendritic-zinc powders at 250 mA cm^{-2} at 25 °C.

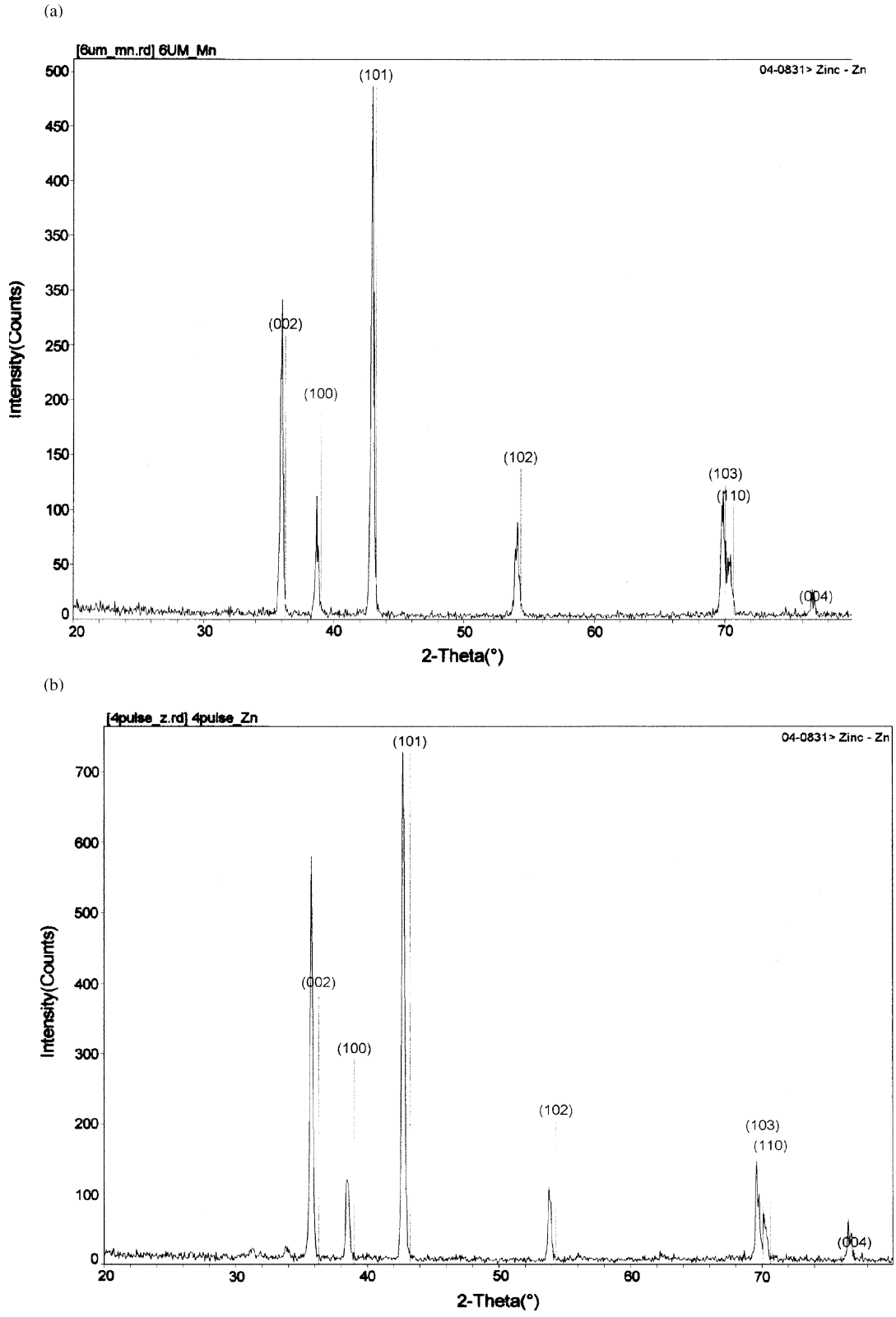

Fig. 2. Microstructure analysis of zinc powder: (a) molten zinc-powder; (b) electrolytic dendritic-zinc powder at 250 mA cm^{-2}.

current efficiency. It is found that the density of the electrolytic zinc powder was increased when the temperature of zinc electrodeposition is increased.

3.2. Surface morphology of electrolytic zinc powder

Electron micrographs of the surface morphology of commercial molten-zinc powder and electrolytic dendritic-zinc powder are shown in Fig. 1a and b, respectively. The molten-zinc powder is composed of oval shaped, cylindrical non-porous particles. By contrast, the electrolytic zinc powder is a dendrite-like (leaf) and, highly porous. The dimension of commercial molten-zinc powder is about 200–500 μm, whereas, the size of the electrolytic dendrite zinc-powder is only 100–150 μm.

3.3. Microstructure of electrolytic zinc powders

X-ray diffractograms for molten-zinc powder and electrolytic dendritic-zinc powder are shown in Fig. 2a and b, respectively. It can be seen that the characteristic (1 0 1), (1 0 0), (0 0 2), (1 0 2), (1 0 3) and (1 1 0) peaks of molten zinc in Fig. 2a are all the same as those of electrolytic dendritic-zinc powder in Fig. 2b. It is obvious, therefore, that the microstructure of electrolytic dendritic zinc is identical to that of molten zinc.

3.4. Impedance analysis of Zn–MnO_2 cells

The ac impedance analyses were carried out prior to and after constant-current discharge experiments. The results for

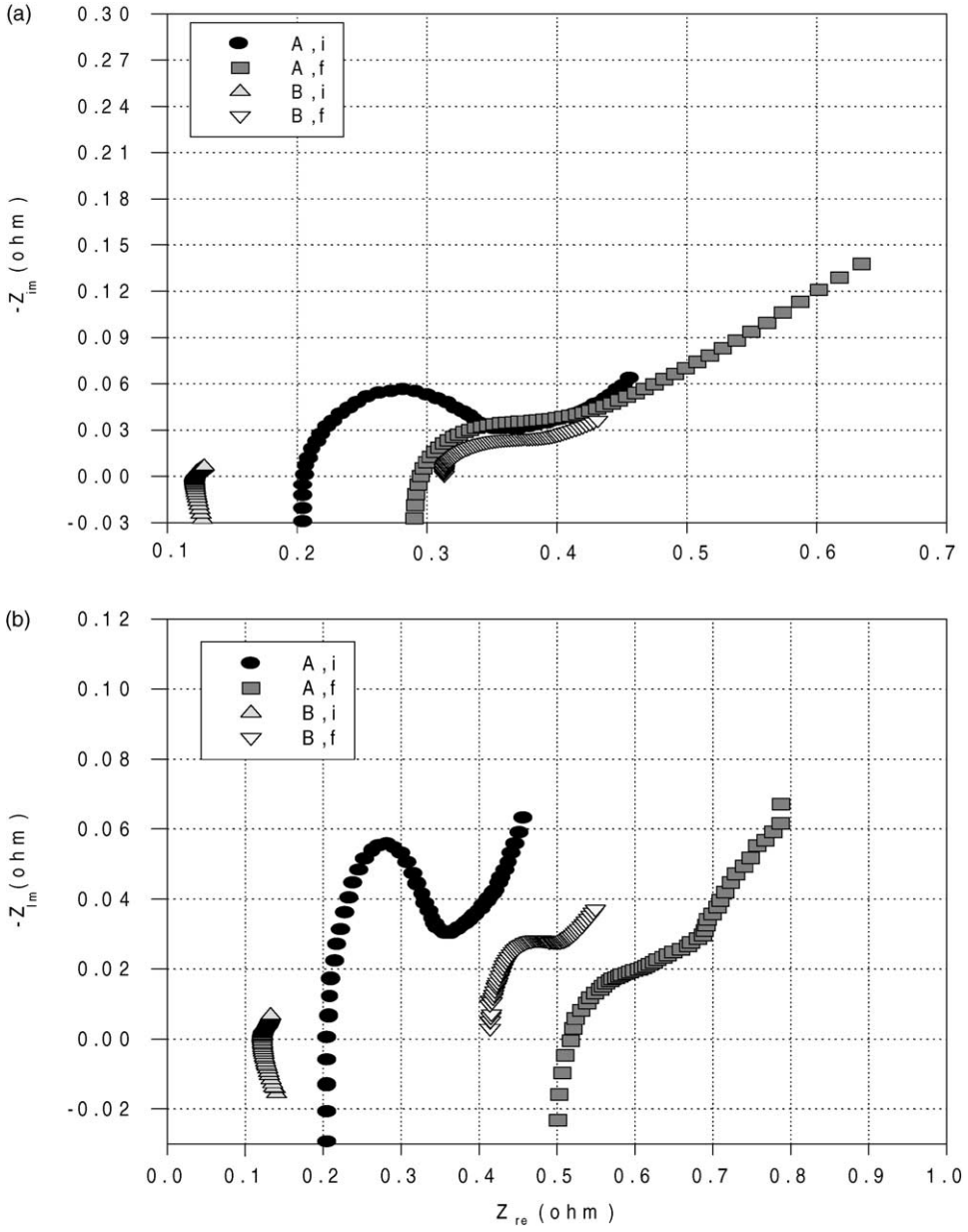

Fig. 3. The ac impedance analysis of LR6 Zn–MnO_2 cells (A: commercial AA cell; B: laboratory cell (with electrolytic zinc)): (a) 200 mA rate; (b) 600 mA rate.

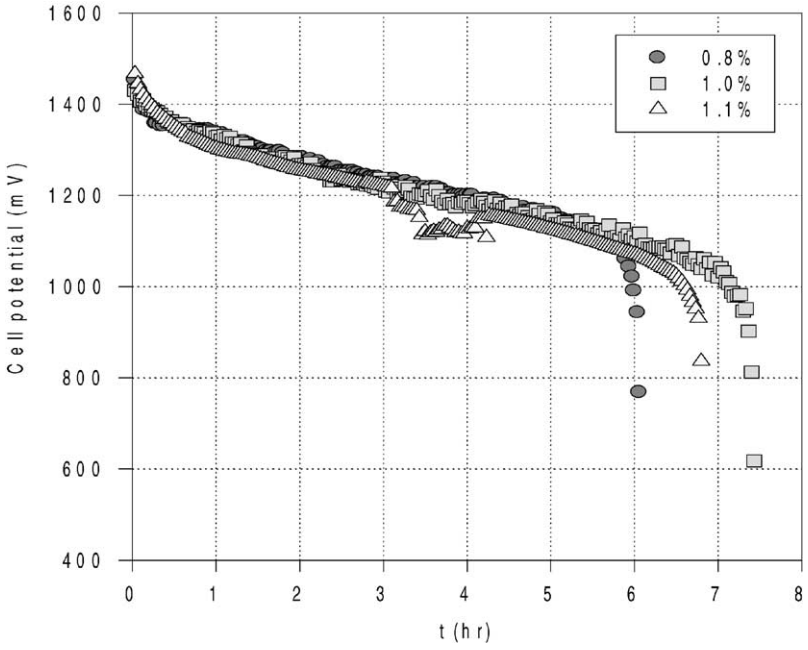

Fig. 4. Effect of gelling agent on performance of laboratory Zn–MnO_2 cells at discharge rate of 200 mA; cell with 20 wt.% electrolytic dendritic-zinc powder in gel.

a commercial Zn–MnO_2 cell and a lab-made LR6 alkaline Zn–MnO_2 cell with electrolytic dendritic-zinc powder in a gel are shown in Fig. 3a and b, respectively. The bulk resistance (R_b) of the cell is determined from the Nquist plot at the point of intersection of the semicircle with the real axis. When the commercial alkaline Zn–MnO_2 cell is discharged at 200 mA, the initial and final bulk resistances are 0.206 and 0.295 Ω, respectively. At a high discharge rate (600 mA), the initial and final bulk resistances of the commercial cell are 0.2059 and 0.518 Ω, respectively. It is apparent that commercial cells display an increase in bulk resistance when discharged at high rates. The initial and final bulk resistances of a laboratory cell made with electrolytic dendritic-zinc powder are 0.121 and 0.206 Ω, respectively at a discharge rate of 200 mA. At the 600 mA rate, the initial and final bulk resistances are 0.122 and 0.414 Ω, respectively.

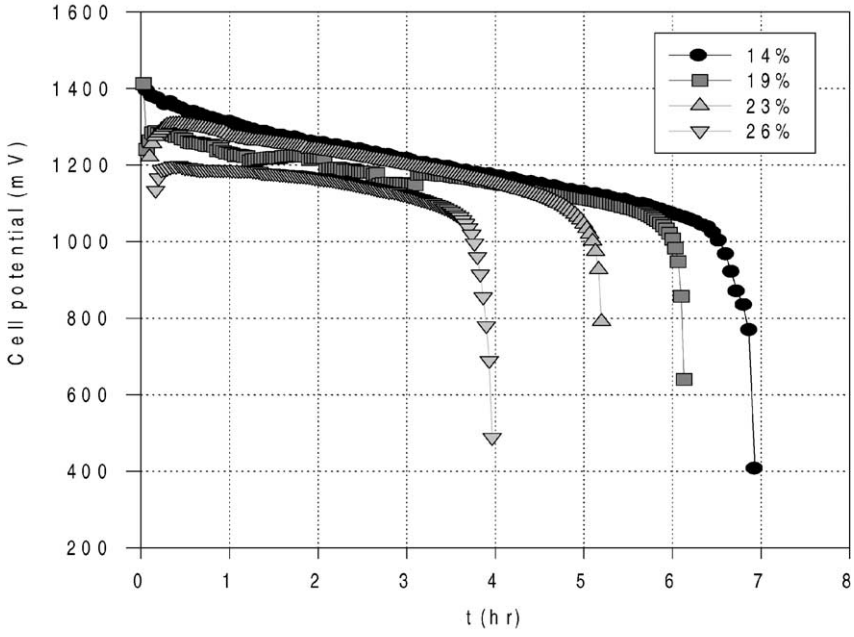

Fig. 5. Effect of water content on performance of laboratory Zn–MnO_2 cells at discharge rate of 200 mA; cell with 20 wt.% electrolytic dendritic-zinc powder in gel.

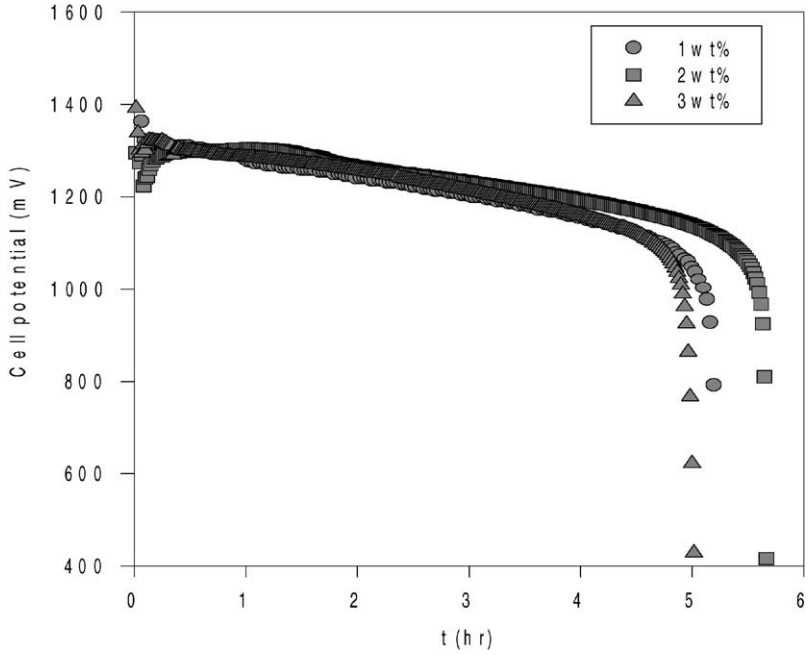

Fig. 6. Effect of ZnO content performance of laboratory Zn–MnO_2 cells at discharge rate of 200 mA at 25 °C; cell with 20 wt.% electrolytic dendritic-zinc powder in gel.

These results show that the impedance of the laboratory cell is much less than that of the commercial cell at a higher discharge rate. The reason for the lower impedance and higher zinc utilisation of laboratory cell may be due to the unique properties of electrolytic zinc powder, namely, high porosity, high surface area and dendrite characteristics, as shown in Fig. 1b.

3.5. Effect of gelling agent on electrochemical performance of Zn–MnO_2 cells

Discharge curves of a LR6 Zn–MnO_2 cell with different weight percentages of gelling agent (Carbopol 940) at a constant current of 200 mA are presented in Fig. 4. The highest utilization of the zinc powder material is 57% at

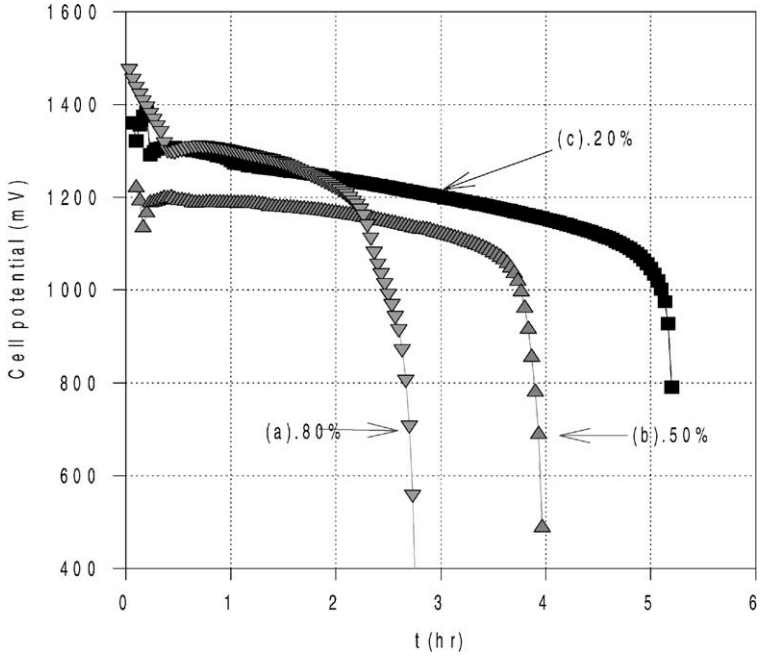

Fig. 7. Effect of content of dendritic-zinc powder on performance of laboratory Zn–MnO_2 cells, at discharge rate of 200 mA at 25 °C: (a) 80 wt.%; (b) 50 wt.%; (c) 20 wt.% electrolyte dendritic-zinc powder in gel.

Table 3
Cell capacity of laboratory alkaline Zn–MnO_2cells at discharge rate of 200 mA

Zinc powder in gel (wt.%)	Zinc in gel (g)	t (h)	Q_{re} (mAh)	E_{avg} (mV)	$R_{b,i}$ (Ω)	$R_{b,f}$ (Ω)	Zinc utilization (%)
20	3.6	5.22	1042	1216	0.3992	0.1786	56.02
50	3.6	3.98	769	1171	0.3962	0.5171	42.80
80	3.6	2.78	554	1270	0.1724	0.2418	29.78

1 wt.% of gelling agent. The utilization of zinc powders with 0.8 and 1.1 wt.% gelling agents in gels is 47 and 52%, respectively.

3.6. Effect of water content in zinc gel

It is believed that the water content in the gel has a significant effect on the electrochemical performance of Zn–MnO_2 cells. Discharge curves of LR6 Zn–MnO_2 cells with water content of 14–26 wt.% at a discharge rate of 200 mA (Fig. 5). It is observed that the maximum utilization of the zinc material is 58% when the cell contains 14 wt.% of water moisture in the zinc gel. Serious leakage problems occur when the water moisture content in the gel is 26 wt.%.

3.7. Effect of ZnO on electrochemical properties of Zn–MnO_2 cell

The ZnO content in the zinc gel has a profound effect on the electrochemical properties of alkaline Zn–MnO_2 cells. Discharge curves of a Zn–MnO_2 cell with 1–3 wt.% ZnO at a discharge rate of 200 mA are given in Fig. 6. The optimum content of ZnO for Zinc utilization is at 2 wt.%. The utilization of zinc powder in the gels decreases when the ZnO content is higher than 3 wt.% or lower than 1 wt.%. It is considered that the electrochemical performance of the cell could be improved when a suitable amount of ZnO is added to the KOH electrolyte solution. The ZnO forms zincate ions in KOH solution. It appears that an increasing concentration of zincate in the KOH electrolyte can prevent the zinc active material from further corroding or dissolving.

3.8. Effect of electrolytic zinc powder on electrochemical properties of Zn–MnO_2 cell

Porous electrolytic dendrite zinc-powder was added to the zinc gel to explore the possibility of an improvement in the electrochemical performance of alkaline Zn–MnO_2 cells. Discharge curves for cells with various compositions of electrolytic dendritic-zinc powder in the gel are given in Fig. 7 for a discharge rate of 200 mA. The highest utilization of zinc powder is 56.02%, for a cell with 20 wt.% electrolytic zinc powder. The utilization for 50 and 80 wt.% electrolytic zinc powder is 42.80 and 29.78%, respectively, as presented in Table 3.

Discharge curves of laboratory Zn–MnO_2 cell with the 20 wt.% electrolytic zinc powder and a commercial cell at a

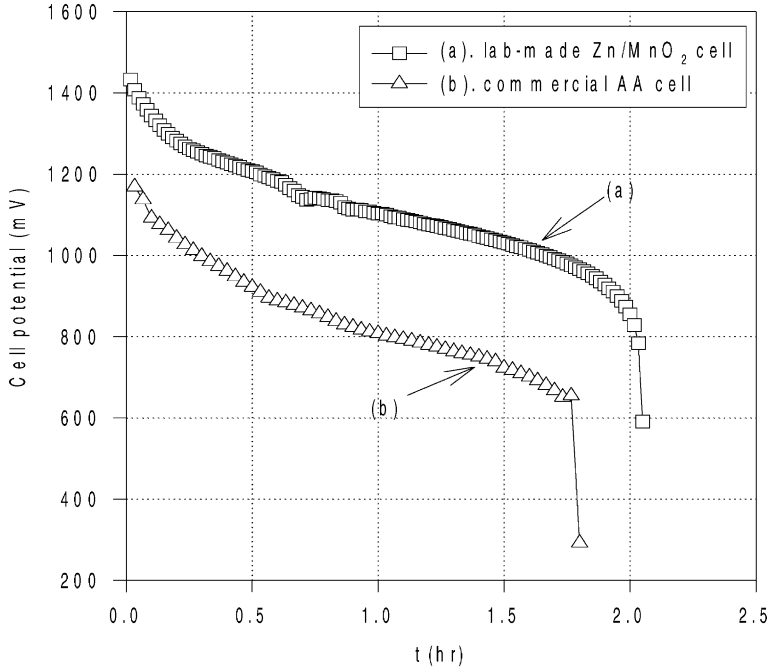

Fig. 8. Comparison of performance of commercial AA cell with laboratory Zn–MnO_2 cell at discharge rate of 600 mA at 25 °C.

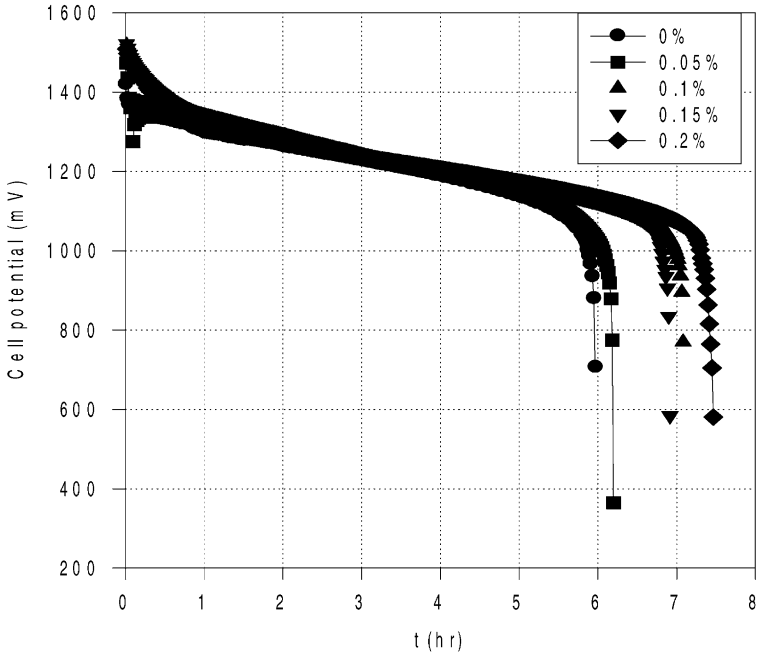

Fig. 9. Effect of content of indium acetate on electrochemical performance of laboratory Zn–MnO_2 cells at discharge rate of 200 mA at 25 °C.

Table 4
Capacity of zinc powder for alkaline Zn–MnO_2 cell at various discharge rates

Current (mA)	Capacity of zinc (mAh g^{-1})	
	Commercial AA cell	Laboratory cell (with 20% electrolytic zinc powder)
50	732.0	715.66
200	545.1	610.1
400	433.4	499.3
600	295.7	462.2

higher discharge rate of 600 mA are given in Fig. 8. The capacity (mAh g^{-1}) of the laboratory cell increases as the discharge rate is increased, as shown in Table 4. Thus, the utilization of zinc is improved at high discharge rates by doping with electrolytic zinc powders.

3.9. Effect of indium acetate on performances of Zn–MnO_2 cell

Indium acetate was used as an inhibitor of hydrogen evolution in the zinc gel [23,24]. Indium can improve the conductivity of electrodes, and reduce the impedance of cell. Hydrogen evolution can be effectively suppressed when a suitable amount of indium acetate is added to the KOH electrolyte. Discharge curves of a Zn–MnO_2 cell with different percentages of this additive (from 0 to 0.20 wt.%) at the 200 mA rate are given in Fig. 9. The maximum utilization of zinc materials, viz. 70%, is shown by a gel with 0.2 wt.% indium acetate.

4. Conclusions

Highly porous, electrolytic dendritic-zinc powders have been prepared from 8 M KOH solution containing 6 wt.% ZnO by a galvanostatic electrodeposition method. The surface morphology and microstructure of the powders are individually studied by using SEM and XRD. The effects of gelling agent, water content, ZnO content, and amount of indium acetate on the electrochemical performances of LR6-size, cylindrical, alkaline Zn–MnO_2 cells are systematically investigated by the ac impedance technique and galvanostatic discharge experiments. It is found that the addition of 20 wt.% electrolytic dendritic-zinc powder to the gel can significantly improve the high-rate discharge capability and also enhance the utilization of zinc active materials.

References

[1] F.R. McLarnon, E.J. Cairns, J. Electrochem. Soc. 138 (1991) 645.
[2] K.A. Striebel, F.R. McLarnon, E.J. Cairns, J. Power Sources 47 (1994) 1.
[3] V. Ravindran, V.S. Muralidharan, J. Power Sources 55 (1995) 237–241.
[4] T.S. Lee, J. Electrochem. Soc. 122 (1975) 171.
[5] J.L. Zhu, Y.H. Zhou, C.Q. Gao, J. Power Sources 72 (1998) 231.
[6] M. Yano, S. Fujitani, K. Nishio, Y. Akai, M. Kurimura, J. Power Sources 74 (1998) 129–134.
[7] E. Frackowiak, J.M. Skowronski, J. Power Sources 73 (1998) 175–181.
[8] B. Szczesniak, M. Cyrankowska, A. Nowacki, J. Power Sources 75 (1998) 130–138.
[9] Y. Shen, K. Kordesch, J. Power Sources 87 (2000) 162–166.

[10] Y. Sharma, M. Aziz, J. Yusof, K. Kordesch, J. Power Sources 94 (2001) 129–131.
[11] J.Y. Huot, M. Malservisi, J. Power Sources 96 (2001) 133–139.
[12] E.J. Podlaha, H.Y. Cheh, J. Electrochem. Soc. 141 (1994) 15.
[13] E.J. Podlaha, H.Y. Cheh, J. Electrochem. Soc. 141 (1994) 28.
[14] J.J. Kriegsman, H.Y. Cheh, J. Power Sources 77 (1999) 127–135.
[15] J.J. Kriegsman, H.Y. Cheh, J. Power Sources 84 (1999) 52–62.
[16] J.J. Kriegsman, H.Y. Cheh, J. Power Sources 84 (1999) 114–125.
[17] J.J. Kriegsman, H.Y. Cheh, J. Power Sources 79 (1999) 262–270.
[18] J.J. Kriegsman, H.Y. Cheh, J. Power Sources 77 (1999) 127–135.
[19] J.J. Kriegsman, H.Y. Cheh, J. Power Sources 85 (2000) 190–202.
[20] Y. Zhang, H.Y. Cheh, J. Power Sources 87 (2000) 174–185.
[21] A.R. Suresh Kannan, S. Muralidharan, K.B. Sarangapani, V. Balaramachandran, V. Kapali, J. Power Sources 57 (1995) 93–98.
[22] D. Pletcher, F.C. Walsh, Industrial Electrochemistry, Blackie, London, UK, 1990, pp. 396–400.
[23] K. Kuwayama, J. Nakagawa, K. Tomii, K. Hagimori, US Patent 4,432,937 (1984).
[24] E. Casey, US Patent 5,780,186 (1998).